Pergamon

Journal of Structural Geology, Vol. 18, No. 9, pp. 1139 to 1149, 1996

0191-8141/96 $15.00+0.00

PII: S0191-8141(96)00045-4

Relative scale and the strength and deformability of rock masses

RICHARD A. SCHULTZ

Geomechanics–Rock Fracture Group, Department of Geological Sciences, Mackay School of Mines/172 University of Nevada, Reno, NV 89557, U.S.A.

(*Received* 31 *March* 1995; *accepted in revised form* 8 *May* 1996)

Abstract—The strength and deformation of rocks depend strongly on the degree of fracturing, which can be assessed in the field and related systematically to these properties. Appropriate Mohr envelopes obtained from the Rock Mass Rating (RMR) classification system and the Hoek–Brown criterion for outcrops and other large-scale exposures of fractured rocks show that rock-mass cohesive strength, tensile strength, and unconfined compressive strength can be reduced by as much as a factor of ten relative to values for the unfractured material. The rock-mass deformation modulus is also reduced relative to Young's modulus. A "cook-book" example illustrates the use of RMR in field applications. The smaller values of rock-mass strength and deformability imply that there is a particular scale of observation whose identification is critical to applying laboratory measurements and associated failure criteria to geologic structures. Copyright © 1996 Elsevier Science Ltd

INTRODUCTION

In many structural geology textbooks and research papers, the mechanical properties of a rock unit containing fractures or faults are inferred from either the intact or fracture strength of small, centimeter-scale samples of rock. Textbooks do not include the concept of rock mass nor do they discuss approaches to solving the scale dependence of intact or sliding-line theories when they are applied to outcrop- and field-scale situations. Similarly, classical rock mechanics textbooks emphasize the elastic, viscous, or plastic rheological equations (e.g. elastic stress–strain relations, relationships between the elastic moduli), used by many geologists and geophysicists, to the exclusion of rock-mass concepts that can be equally or more applicable to large, polyphase, discontinuous rock exposures. A knowledge of rock masses and scale-dependent idealizations is useful for structural geologists working in regions of active or near-surface tectonics or in any fractured rock unit.

This paper summarizes a method, well known in geological and mining engineering, for characterizing the mechanical properties of outcrop-scale (and larger) rock units; it can complement traditional techniques of structural geology. The *rock mass* is an aggregate material consisting of both intact rock and the associated joints, faults, bedding planes, solution surfaces, and other discontinuities. The concept of rock masses, and the associated classification schemes for incorporating the influence of fracture networks, is a powerful tool for estimating and understanding large-scale rock properties, and it has direct applications to field and theoretical structural geology. Attention is focused here on brittle behavior, although other important processes (quasi-plastic, viscous) can contribute to rock mass deformation at particular scales of length and/or time. Following a brief review of rock failure criteria, a rock-mass characterization is presented using cooled basaltic lava flows as an example. Elastic stresses due to subsurface dike inflation, when compared to the failure criteria, illustrate an application of rock-mass concepts to a problem in active tectonics.

BRITTLE STRENGTH CRITERIA FOR ROCKS

A Mohr envelope for intact rock (Jaeger & Cook 1979) may be idealized as linear (Coulomb criterion), parabolic (Griffith criterion), or some combination of these (Modified Griffith criterion) over a given range of normal and shear stresses (Fig. 1). The envelopes are

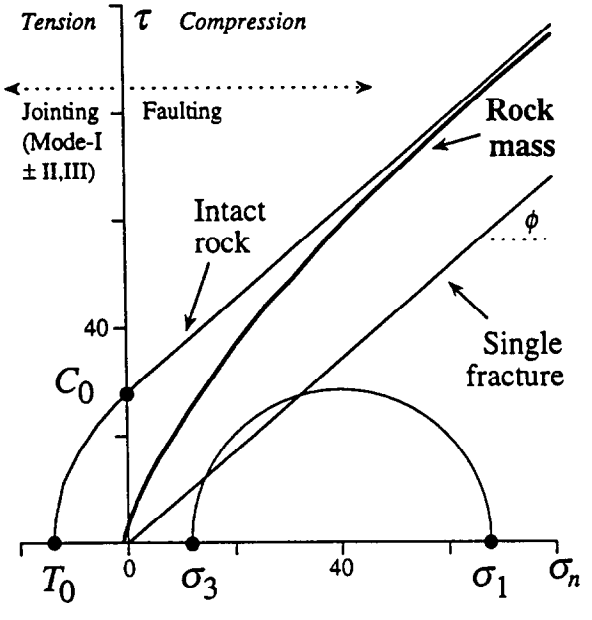

Fig. 1. Mohr diagram showing commonly used representations of intact and fractured rock strengths and the influence of relative scale on strength criteria. The intact envelope, consisting of a parabolic Griffith envelope for tensile normal stress and a linear Coulomb envelope for compression, assumes that microcracks and other flaws are minute compared to the size of the rock specimen. The 'sliding-line' envelope (Byerlee's rule), defined by the frictional properties of a single joint, fault, or artificial saw-cut surface, implies that a single fracture plane completely cuts the rock. Rock-mass response can fall between these two extremes.

constructed using values for tensile strength T_0, cohesive strength C_0, and internal friction $\mu = \tan \phi$, where ϕ is the friction angle, obtained from testing of small intact samples. Envelopes based on these intact-rock values can be inappropriate for outcrops and larger volumes because they ignore the weakening effects of fractures (e.g. Hoek 1983). An inverse relationship between size and strength, well known for engineering (Griffith 1921) and geological (e.g. Scholz 1990, pp. 28–29) materials, can be attributed to flaws or fractures in the material.

The shear strength of fractures (joints and faults) is normally given by a linear Coulomb criterion (Byerlee 1978, now referred to as Byerlee's rule by Kohlstedt *et al.* 1995) with smaller values of cohesive strength and friction than those used for the intact rock material. This single-plane-of-weakness model (Priest 1993) assumes that a fully developed, continuous fracture completely cuts the sample or outcrop. The strengths of anisotropic rocks (e.g. shales, schists, and rock domains containing sets of parallel faults) can also be idealized succinctly by comparing the intact and fractured strengths on a Mohr diagram (Fig. 1). Although faults can appear to completely cut an outcrop, an orogenic belt, or the Earth's crust, faults and joints are discontinuous at a particular scale of observation (e.g. Aydin 1988, Pollard & Aydin 1988). The simple Coulomb criterion defined for small, cm-scale rock surfaces can underestimate the frictional strength of the entire fault or fracture array unless the rock-bridge strength (unbroken rock between discontinuous fracture segments) and other factors are also included (Patton 1966, Priest 1993). For example, Barton's (Barton 1990) equation for joint friction angle (equation (1)):

$$\phi = JRC^* \log\left(\frac{\sigma_c^*}{\sigma_n}\right) + \phi_0 + i \qquad (1)$$

includes additional scale-dependent surface roughness properties (scale-dependent joint roughness coefficient, JRC^*; unconfined compressive strength of rock mass, σ_c^*; large-scale waviness angle of surface, i) beyond the basic friction angle ϕ_0 (given by Byerlee's rule). Rough or wavy fractures have greater frictional resistance than do smooth planar ones in the same rock. Barton's criterion is commonly used in engineering design studies to estimate the frictional strength of outcrop-scale fracture surfaces, although the corrections to Byerlee's rule appear to be relatively small for many faults (Sibson 1994).

Byerlee's rule assumes dry, unaltered rock surfaces, although the friction of certain hydrous clay minerals can be much lower (i.e. $\mu \approx 0.3$) for the same low-pressure range (Byerlee 1978). Gouge formation (Marone 1995), alteration of fracture surfaces as well as coatings by secondary minerals such as calcite and serpentine, and groundwater circulation through fracture networks, can all promote reductions in frictional strength. As a result, rock types such as hydrothermally altered pyroclastic tuff (see below) can be weaker than Byerlee's rule in near-surface exposures.

The classical strength criteria (Griffith, Coulomb) should only be used to estimate or constrain the properties of geologic materials within their respective ranges of applicability. For example, a Griffith or Griffith-type criterion should be used only for rocks in which no macroscopic fracturing is visibly apparent *at the scale of observation.* Byerlee's rule should only be applied to *portions* of fractures. Rock exposures, whether hand samples, outcrops, or crystal sections, which contain discontinuous fractures that are *significant at the scale being considered* are best characterized by a rock-mass criterion. Measurements of in-situ stresses in rocks shallower than ~1 km depth can be highly variable (e.g. Plumb 1994), reflecting significant contrasts in rock-mass properties such as lithology, fracturing and local stress state at that scale (Brady & Brown 1992). Below this depth, Byerlee's rule, suitably adjusted for pore-fluid pressure, provides a satisfactory fit to the in situ stress measurements and a rock-mass description of crustal and lithospheric rock (e.g. Kohlstedt *et al.* 1995) may no longer be appropriate (Amadei *et al.* 1988).

Relative scale is defined here as the ratio of scale of observation to scale of fracturing. Rock mass behavior, and appropriate choices of strength criteria, are scale dependent (Heuzé 1980, Angelier 1989). A rock unit is considered here to be *continuous* for a given relative scale when discontinuity characteristics (e.g. length, spacing) are statistically constant, leading to homogeneous properties (Priest & Hudson 1981). Rock units with spatially variable properties (fracturing, block size) at a given scale are *discontinuous.* Consider a basaltic lava flow characterized by three-dimensional networks of cooling fractures having crack lengths of centimeters to meters. For a scale of observation of millimeters to centimeters, the flow can be considered as intact basaltic rock and idealized by those properties. At significantly smaller scales, grain size and microcracks become important enough that the assumption of a continuous material may not apply. For a scale of meters the rock unit can be described as intact basalt partly separated into irregular blocks by numerous discontinuous fractures. This scale of observation is comparable to the scale of fracturing. (or, equivalently, block size) and none of the continuum models for intact rock material, joint slip, or rock-mass strength discussed above apply (Hoek 1983). Discontinuum methods such as keyblock theory (Goodman & Shi 1989, Goodman 1995) for the aggregate material should be used instead. At dimensions for which the scale of observation greatly exceeds (e.g. by a factor of 5–10) the block size or fracture spacing, the lava flow can be described as an equivalent continuum (Priest 1993) and a rock mass. A 10-cm basaltic rock core and 10-m outcrop are both continuous (or intact) *at the relative scale* although the specific parameters for strength and deformability differ for each (intact vs rock mass). The concept of relative scale is fundamental given that other properties such as fracture toughness, stability and critical slip distance of frictional sliding, and hydraulic permeability for rock masses, can differ markedly from values for small intact laboratory samples.

CHARACTERIZATION OF THE ROCK MASS

Probably the most widely used approach to representing the response of fractured rock to stress is that proposed by Hoek & Brown (1980) (see also Bieniawski 1989 and Brady & Brown 1992 for detailed procedures). Application of this two-part empirical criterion to fractured rock units is straightforward in concept but often challenging in practice. However, the procedure can often be accomplished in the field using the methods outlined below. The Hoek–Brown criterion can be applied most directly to rock units that approximate isotropic behavior, such as basalts and tuffs having three-dimensional fracture sets. For anisotropic units (e.g. one joint set) the criterion can be modified for fracture set orientation. In the first part, rock-mass properties are characterized systematically by using a rock-mass classification system (Rock Mass Rating System (RMR), Bieniawski 1989) that captures the major elements of fracture frequency, spacing, condition (weathered or rough), groundwater conditions, and intact-rock strength. RMR is an empirical system based on >350 case histories of successful rock mass design in tunnels, underground chambers, mines, slopes, and foundations in many different rock types and tectonic settings. The second part involves calculation of the Hoek–Brown rock-mass strength parameters (for the Mohr envelope) and deformation modulus, E^* (corresponding to Young's elastic modulus E), from the values of RMR; these parameters, in turn, allow useful strength properties for the fractured exposure (such as tensile strength) to be calculated.

Jointed basaltic rocks such as those found on the Columbia Plateau in Washington State provide examples of a highly fractured rock mass with a high Young's modulus for the intact rock (e.g. Schultz 1995). A complementary example is that of Calico Hills tuff, a highly fractured rock mass characterized by low-modulus rock (Schultz & Li 1995). The tuff consists primarily of pyroclastic airfall material that was locally reworked into bedded sequences (e.g. Lin *et al.* 1993). Calico Hills tuff underlies the Topopah Spring Member of the Miocene Paintbrush Tuff, which is currently undergoing engineering evaluations for the proposed high-level nuclear waste repository at Yucca Mountain, Nevada. The Topopah Spring Member is a densely welded tuff that represents a useful intermediate example. Determination of RMR for a basaltic rock mass (Table 1), succinctly illustrates the method; rock-mass characteristics for the two tuffs are taken from the literature to facilitate comparison between these rock types. Note that all categories listed in Table 1 that contribute to RMR, except for intact-rock strength, can be determined easily in the field.

Procedure

The first step is to characterize the fracture population. The procedure is documented in Fig. 2 following Bieniawski (1989). Three main categories, or rock-mass *index properties*, of intact rock strength (unconfined or uniaxial compressive strength, σ_c) (row 1 in Fig. 2), fracture or discontinuity characteristics (rows 2a, 2b, and 2c), and groundwater conditions (row 3) are assessed either in the laboratory or in the field as appropriate. A computed value of RMR from 0 (completely fractured, very weak and hydrothermally altered) to 100 (rare fractures, pristine), obtained by summing the contributions of each category, is then determined for the rock mass, which must also have minimum dimensions of several meters in this approach. Figure 2 can be added to a field notebook to aid in real-time characterization of a given rock mass; tentative values for intact-rock strength can be assigned in the field and later verified by laboratory tests.

Fracture spacings in the outcrop are traditionally assessed for two ranges of scale, centimeter and meter. The small-scale spacing (cm and smaller) is established either from core, using RQD (rock quality designation, Deere 1963 and Appendix), or from the outcrop face, by counting the number of fractures that intersect a tape measure placed on the outcrop and dividing by tape length (e.g. 1 m). This small-scale spacing, or linear fracture density N, is converted to the equivalent RQD value by using the empirical expression

$$\mathrm{RQD} = 100e^{-0.1N(0.1N+1)} \tag{2}$$

in which N is the number of fractures per meter length (Brady & Brown 1992, p. 54). The large-scale spacing is obtained from an outcrop traverse similar to the previous one, but with measured spacings in the range of centimeters and larger. In this case the spacings are not normalized by traverse length but are averaged, and then recorded, in units of meters (see Fig. 2). Because the RMR classification system is itself only approximate, none of the categories listed in Fig. 2 need be determined precisely. In fact, ballpark values or initial guesses to parameters such as compressive strength, made in the field and refined later, can provide a rapid and reliable first-approximation of the strength and deformability of the rock mass.

The broad categories shown in Fig. 2 provide useful values of RMR. For example, the range of RMR illustrated in Table 1 for the basalt, 58–67, reflects the uncertainty in discontinuity and groundwater conditions in the lithologic description provided (Table 1, top). While a more detailed classification is possible (Bieniawski 1989), the ranges determined in Table 1 are sufficient to illustrate the significant differences in mechanical properties between an intact rock and its fractured rock mass. The deformation modulus (AKA effective stiffness, effective Young's modulus for a cracked material) can be computed directly from RMR (Table 2) for RMR less than or greater than 50 (Fig. 3).

Values of RMR are associated with the Hoek–Brown failure criterion by calculating the unnamed, dimensionless Hoek–Brown parameters m and s that reflect the degree of block interlocking and fracturing of the rock

Table 1. Example of RMR determination

	Field Observations
Rock:	Fine-grained tholeiitic continental flood basalt; Grande Ronde, WA, basalt, Hanford site
Intact strength:	~ 150 to 350 MPa (uniaxial compression test); $m_i = 22$; $s = 1.0$; $C_0 \approx 66$ MPa; $T_0 \approx -15$ MPa
Rock mass:	Jointed prismatic blocks typically ≤ 2.4 m tall by < 0.5 m in diameter
RQD:	60% from vertical core or outcrop spacing
Joint sets:	Vertical, variety of strikes; and horizontal
Joint roughness:	Smooth to rough, coatings of secondary minerals
Water:	May saturate rock mass
	Synthesis of Field Properties
Rating for uniaxial compressive strength:	15
Rating for RQD:	13
Rating for discontinuity spacing:	10
Rating for discontinuity condition:	20–25
Rating for groundwater conditions:	+ 0–4
Rock Mass Rating =	58–67
	Field and Office Calculations
Deformation modulus E^*[a] =	16–34 GPa
Hoek–Brown parameter m =	4.91–6.77
Hoek–Brown parameter s =	0.0094–0.026
Rock-mass unconfined compressive strength $\sigma_c{}^*$[b] =	14.5–56.4 MPa
Rock-mass tensile strength $T_0{}^*$ =	−0.29 to −1.3 MPa
Rock-mass cohesive strength $C_0{}^*$ =	1.2–3.5 MPa

[a]Deformation modulus E^*, m, and s calculated using upper and lower values for RMR.
[b]Rock-mass unconfined compressive, tensile, and cohesive strengths calculated using ranges of intact strength values, m, and s.

mass (Fig. 4). Conversion relationships are given by

$$m = m_i \exp\left(\frac{\text{RMR} - 100}{28}\right) \quad (3)$$

$$s = \exp\left(\frac{\text{RMR} - 100}{9}\right) \quad (4)$$

in which m_i is the value for the intact rock material obtained from a laboratory test or published table (Bieniawski 1989, Priest 1993). The non-intuitive parameter m depends on rock type and decreases with the degree of (prefailure) fracturing or blockiness of the rock mass; for $s = 1$ and $m_i >> 1$, m_i approximates the ratio between the uniaxial compressive strength and tensile strength of the intact rock (Hoek & Brown 1980). On a Mohr diagram, large values of m or m_i (e.g. 15–25, hard crystalline rocks) promote steeply inclined Mohr envelopes with high instantaneous (normal-stress dependent) friction angles at low effective stress levels, whereas low values of m or m_i (e.g. 3–7, softer sedimentary rocks) promote lower instantaneous friction angles (Hoek 1983). Representative values include $m_i = 7$ for intact limestone and carbonate rocks, $m_i = 10$ for lithified argillaceous rocks (shales), $m_i = 15$ for sandstones and quartzite, $m_i = 17$ for fine-grained igneous rocks, $m_i \geq 25$ for coarse-grained crystalline igneous and metamorphic rocks. For intact rock, $s \equiv 1$ and for pervasively fractured rock, $s \equiv 0$; values for typical rock masses fall within these extremes (Fig. 4a). Decreases in s cause the Mohr envelope to shift downward slightly, to smaller values of shear stress, with negligible change in shape of the envelope. Note that the tensile strength of a pervasively fractured rock mass with $s = 0$ is zero (Table 2). Because most rock masses have small values of s (e.g. < 0.1), the tensile strength of large, discontinuously fractured rock exposures is considered by engineers to be negligibly small. Further discussion of these parameters can be found in Hoek (1983), Brown & Hoek (1988), and Bieniawski (1989).

Deformability and strength

Young's (elastic) modulus E is strictly appropriate only for an intact rock sample because E varies inversely with crack density (Walsh 1965, Kulhawy 1975, Segall 1984, Kachanov 1992). Thus the deformation modulus E^* of a rock mass is less than the Young's modulus for the intact rock material (except for the special case of intact rock, where E^* is not well defined). Empirical relationships between RMR and E^* (Table 2, Fig. 3) were found by Bieniawski (1989) and others to be relatively insensitive to rock type, paralleling the findings of Byerlee (1978) and others that the shear strength of individual planes in rock also varies little with rock type. The more fractured a rock unit becomes, the less its modulus depends on rock type, so that these relations become more reliable as fracture density increases (and RMR decreases). Case studies compiled by Bieniawski (1989) suggest about a $\pm 20\%$ error in calculated vs in-situ measurements of E^* for the full range of RMR for a variety of high-modulus rock types ($E > 10$ GPa). Poisson's ratio υ does not appear to vary systematically with RMR, according to similar in situ measurements. Shear modulus G^* for the rock mass should also be lower than G for the (isotropic) intact rock material, given $G = E/2(1 + \upsilon)$ for elastic loading and similar relationships for anisotropic materials.

Predicted values for deformation modulus of fractured basalt and tuff exposures agree well in many cases with actual in situ measurements on large samples (Fig. 3). For a given range of RMR for fractured welded tuff and basalt (horizontal extent of boxes in Fig. 3), the measured values of E^* for basalt are reasonably well predicted by the empirical relationships. The in situ deformation

	Parameter		Range of Values (component of RMR)							Total:
1.	Strength of intact rock	Point-load index, MPa	> 10	4–10	2–4	1–2				
		Uniaxial compressive strength, MPa	> 250	100–250	50–100	25–50	5–25	1–5	< 1	
	Rating:		15	12	7	4	2	1	0	0–15
2a.	Drill core quality RQD, %		90–100	75–90	50–75	25–50	< 25			+
	Rating:		20	17	13	8	3			3–20
2b.	Spacing of discontinuities, m		> 2	0.6–2	0.2–0.6	0.06–0.2	< 0.06			+
	Rating:		20	15	10	8	5			5–20
2c.	Condition of discontinuities		Very rough Discontinuous No separation Unweathered	Rough walls Separation < 0.1 mm Slightly weathered	Slightly rough Separation < 1 mm Highly weathered	Slickensides *or* Gouge < 5 mm thick *or* Separation 1–5 mm. Continuous	Soft gouge > 5 mm thick *or* Separation > 5 mm. Continuous Decomposed wall rock			+
	Rating:		30	25	20	10	0			0–30
3.	Ground-water	Inflow per 10 m tunnel length, l/min.	none	< 10	10–25	25–125	> 125			
		λ	0	< 0.1	0.1–0.2	0.2–0.5	> 0.5			
		General conditions	Completely dry	Damp	Wet	Dripping	Flowing			+
	Rating:		15	10	7	4	0			0–15

RMR = 1 + 2a + 2b + 2c + 3 ≤ 100

Fig. 2. Chart showing rock-mass classification parameters and their ratings (shaded), after Bieniawski (1989). Values of each parameter (e.g. strength of intact rock) from laboratory or field measurement are compared to the reference values in each row; the rating for each parameter is obtained by reading down to the shaded box. Individual ratings are summed to obtain RMR. λ is the ratio of pore-fluid pressure to the greatest compressive principal stress, σ_1.

moduli for large (> 1 m) blocks of welded Topopah Spring tuff span a narrower range of values (14–33 GPa, Lin *et al.* 1993) than the empirical relationship would predict, except for RMRs < 70. However, both the deformation moduli for both rock types are significantly less, by about a factor of two, than the Young's moduli for the respective intact rock material (73 GPa for the basalt (Schultz 1995), 33–38 GPa for the welded tuff), supporting the use of Bieniawski's empirical relation as a first approximation to the deformability of a fractured rock mass. The deformation modulus for soft, non-welded Calico Hills tuff is not well predicted by Bieniawski's relation, given that this relation is defined and used only for high-modulus rock types.

Strength characteristics of the rock mass can be calculated from the Hoek–Brown criterion. Appropriate values for rock-mass unconfined (uniaxial) compressive strength, tensile strength, cohesive strength, and normal and shear stresses for the Mohr envelope (Fig. 1) listed in Table 2 are obtained directly from the Hoek–Brown equations (Schultz 1995, Table 2). Although many structural geologists may not require such precise values, these diagrams (Fig. 4) illustrate the profound influence of fracturing, and fracture-related processes such as alteration, on rock mass strength. Increased fracturing (or other factors than can reduce RMR, Fig. 2) reduces the Hoek–Brown parameter m relative to m_i for the intact rock material (Fig. 4a), implying that fracturing decreases the slope of the Mohr envelope and the associated instantaneous friction coefficient of the rock

Table 2. Equations for rock masses

Property	Symbol	Expression
Biaxial strength, MPa		$\sigma_1 = \sigma_3 + \sqrt{m\sigma_c\sigma_3 + s\sigma_c^2}$
Hoek–Brown parameter	m	$m = m_i \exp\left(\frac{\text{RMR} - 100}{28}\right)$
Hoek–Brown parameter	s	$s = \exp\left(\frac{\text{RMR} - 100}{9}\right)$
Unconfined compressive strength	σ_c^*, MPa	$\sigma_c^* = \sqrt{s\sigma_c^2}$
Tensile strength	T_0^*, MPa	$T_0^* = \frac{\sigma_c}{2}\left(m - \sqrt{m^2 + 4s}\right)$
Normal stress	σ_n, MPa	$\sigma_n = \sigma_3 + \frac{\tau_{\max}^2}{\tau_{\max} + \frac{m\sigma_c}{8}}$, $\tau_{\max} = \frac{\sigma_1 - \sigma_2}{2}$ [a]
Shear stress	τ, MPa	$\tau = \left(\frac{\tau_{\max}^2}{\tau_{\max} + \frac{m\sigma_c}{8}}\right)\sqrt{1 + \frac{m\sigma_c}{4\tau_{\max}}}$
Cohesive strength ($\sigma_n = 0$)	C_0^*, MPa	$C_0^* = \sigma_c\left(\frac{\sqrt{m^2 + 16s} - m}{4}\right) \cdot \sqrt{\sigma_c^2 + \frac{16m\sigma_c}{(4\sqrt{s} - m + \sqrt{m^2 + 16s})^2}}$
Cohesion intercept ($\sigma_n > 0$)	C_0^*, MPa	$C_0^* = \tau - \sigma_n \tan\phi^*$
Friction angle (σ_n arbitrary)	ϕ^*, degrees	$\phi^* = \tan^{-1}\left[\left\{4h\cos^2\left[30° + \frac{1}{3}\sin^{-1}(h^{-3/2})\right] - 1\right\}^{-1/2}\right]$, $h = 1 + \frac{16(m\sigma_n + s\sigma_c)}{3m^2\sigma_c}$
Joint-to-fault transition stress	σ_{3trans}, MPa	$\sigma_{3\,trans} = \frac{1}{4}(m\sigma_c - \sqrt{m^2\sigma_c^2 + 16\sigma_1^2})$
Deformation modulus	E^*, GPa	$E^* = 2\,\text{RMR} - 100$, (RMR > 50), $E^* = 10^{(\text{RMR} - 10)/40}$, (RMR < 50)

[a] $\tau_{\max} = \frac{\sigma_1 - \sigma_3}{2}$

mass. The parameter s also decreases with decreasing RMR, leading to smaller values of shear stress for a given value of normal stress.

Strength parameters for Calico Hills tuff ($67 \leq$ RMR ≤ 77), Topopah Spring tuff (unit TSw2 of Lin *et al.* 1993, $62 \leq$ RMR ≤ 82), and a range of basalts ($45 \leq$ RMR ≤ 75, Schultz 1995) were calculated using the relationships given in Table 2, and plotted in Fig. 4(b). The tensile strength of the welded tuff is reduced from about -20 MPa, for the intact rock material, to only -1.2 to -5.1 MPa, depending on the RMR of the rock mass. The basaltic rock mass is also weaker in tension, -0.2 to 2 MPa, than the intact basalt, -14 MPa. Similarly, the unconfined compressive strengths are reduced by comparable amounts, from about 160 to 20–60 MPa for the welded tuff, and from 260 to 10–65 MPa for the basalt. Cohesive strengths of the rock masses are also reduced significantly. These strength values allow the Mohr envelope (Fig. 1) and failure characteristics of fractured rock masses to be defined semi-quantitatively.

Mohr diagrams

Mohr envelopes for welded and nonwelded tuff, compared in Fig. 5, demonstrate that the large-scale (e.g. outcrop scale and greater) strengths of the tuff are significantly different than those which are based on the properties of either intact or fractured rock. Hatchured regions in Fig. 5 illustrate the variability in failure envelopes for the tuffs given the ranges in RMR noted above. Corresponding Mohr envelopes for basaltic rocks are given by Schultz (1995). The slopes of the rock-mass envelopes for welded tuff ($\sigma_n < 20$ MPa) are comparable to Byerlee's rule, implying similar values of friction angle (30–35°) or coefficient ($0.6 < \mu < 0.85$). However, the Calico Hills rock mass exhibits much lower angles or

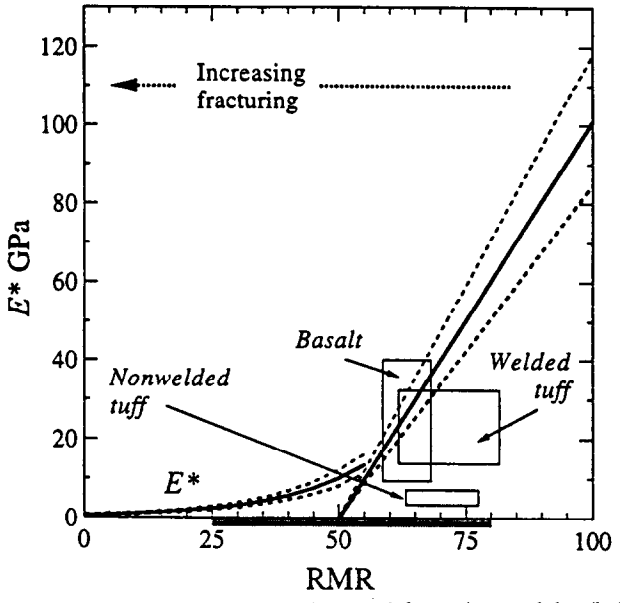

Fig. 3. Predicted variation in rock-mass deformation modulus (bold, dashed curves) with RMR (Table 2, last equations) compared to in situ determinations. Boxes illustrate ranges of measured deformabilities for given rock types and their RMRs; E^* for nonwelded tuff is not well predicted for this soft rock type, given $E < 10$ GPa.

coefficients of friction throughout the full range of normal stress, on the order of 10–15° and $0.2 < \mu < 0.3$ respectively. Note also that the Mohr envelopes for the rock masses are nonlinear, so that instantaneous (normal-stress dependent) friction coefficient and cohesion intercept vary with confining pressure and, therefore, depth.

A transition from jointing to faulting in crystalline rocks can occur when the remote, or regional, normal stress resolved on an array of favorably oriented fractures changes from tensile to compressive (Horii & Nemat-Nasser 1985). On the Mohr diagram (Fig. 1), this point corresponds to the intersection of Mohr circle and failure envelope on the τ-axis. For a given value of σ_1, the transition can be predicted by calculating appropriate values of least principal stress σ_{3trans} (Table 2). Jointing can be predicted if σ_3 at failure is less than σ_{3trans}; faulting can be predicted if σ_3 exceeds σ_{3trans}. Mixed-mode cracking, associated with tensile and shear tractions resolved on a crack and tangency to the envelope in the tensile-stress regime, can evolve into a more regular array of mode-I cracks or joints under conditions of remote normal tension. The continuum-based prediction of failure under tension and shear, using a Mohr envelope, only applies to the initial conditions such as oblique dilation and wing-crack development (Pollard & Aydin 1988) and must be supplemented by an analysis of the stability of these cracks before equating tangency on a Mohr diagram with progressively developed field-scale structures (Schultz & Zuber 1994).

Application to field problems

Schultz & Watters (1995) recently used the criteria presented in this paper to reevaluate models for elastic

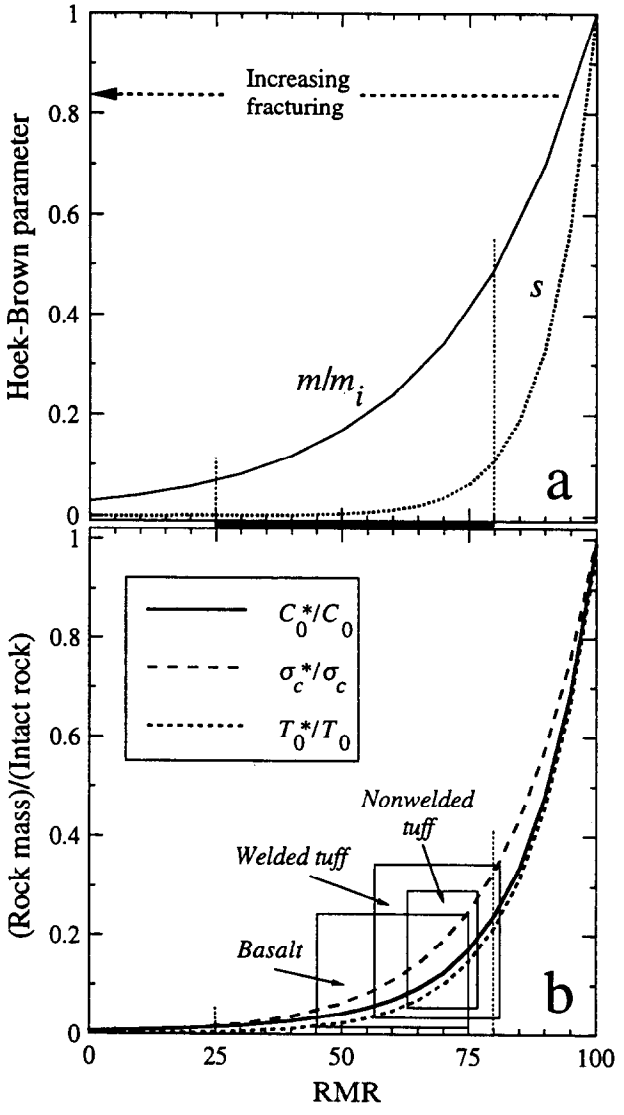

Fig. 4. Dependence of (a) Hoek–Brown parameters m and s (b) rock-mass strength paramters on RMR. Bar and dotted vertical lines show typical range of RMR for rock masses. Boxes show predicted ranges of strength parameters for given ranges of RMR.

buckling of basalts on the Columbia Plateau of Washington State. Previous work assumed a simple Coulomb-frictional strength criterion along with intact-rock values of Young's modulus for the basaltic layer; as a result, calculated values of the critical stress for buckling and modulus contrast between the basaltic plate and sedimentary substrate were implausibly large. Incorporation of rock-mass strength criteria and the smaller value of deformation modulus appropriate to fractured basaltic lava flows (Schultz & Watters 1995) reduces modulus contrasts and the critical stress for buckling to reasonable levels, permitting buckling as a viable mechanism for Yakima ridge formation.

The following example illustrates an application of rock-mass concepts to active extensional tectonics. Dilation of a subsurface igneous dike, and its propagation, represent an important and common deformation event near the Earth's surface (e.g. Rubin 1995). Dike dilation is modeled here by a two-dimensional boundary element method (details of the numerical technique are

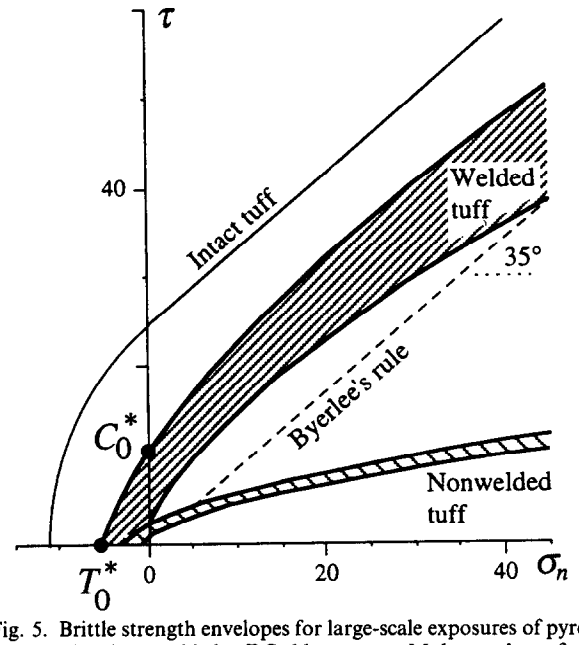

Fig. 5. Brittle strength envelopes for large-scale exposures of pyroclastic welded and nonwelded tuff. Bold curves are Mohr envelopes for rock mass; ranges given by empirical uncertainites in rock-mass properties. Dotted line is Byerlee's rule for pre-existing fractures (arbitrary dry unweathered lithology) assuming $C_0 = 0$ and coefficient of friction of 0.85; curve appropriate for $\sigma_n > 5$ MPa. Solid line is a representative envelope for small intact sample of nonwelded Calico Hills tuff.

given by Crouch & Starfield 1983 and Schultz 1992). The dike is much longer along its strike-length than its depth extent, shown in Fig. 6. The dike extends from 100-m depth down to 1.1-km depth. Remote stresses acting on the dike are the vertical (principal) compressive stress due to overburden, $\sigma_v = 19$ MPa km^{-1}, and least horizontal compressive stress $\sigma_h = 0.5\ \sigma_v$. An internal magma pressure of $2.5\sigma_h$, acting on the interior dike walls, counteracts the horizontal compression, dilates the dike, and changes the state of stress within a few dike widths of the dike and particularly near the Earth's surface. Other pressure distributions within the dike (e.g. Rubin 1995) that could be imposed would not greatly change the conclusions. The dike is imbedded in an elastic half-space having values of Young's modulus of 75 GPa (to simulate intact basaltic rock) or 30 GPa (basaltic rock mass, RMR = 65) and a Poisson's ratio of 0.25.

Given the same values of remote stress and internal pressure, the maximum dike dilation, occurring just above its center, is calculated to be either 0.09 m in the intact rock or 0.23 m in the rock mass (Fig. 6a). The dike in the rock mass dilates 2.5 times more than the dike in intact rock given the smaller value of (deformation) modulus for the surrounding rock mass. Calculation of the opening-mode stress intensity factor (Schultz 1988) at the shallow dike tip, $K_I = 1.85$ MPa m$^{1/2}$, along with a limiting value of fracture toughness for basalt K_{Ic} of about 2–3 MPa m$^{1/2}$, implies for the stated conditions that the dike should not propagate toward the surface; fissuring may occur at the surface away from, and parallel to, the dike (Mastin & Pollard 1988) if the stresses are sufficient to cause fracturing.

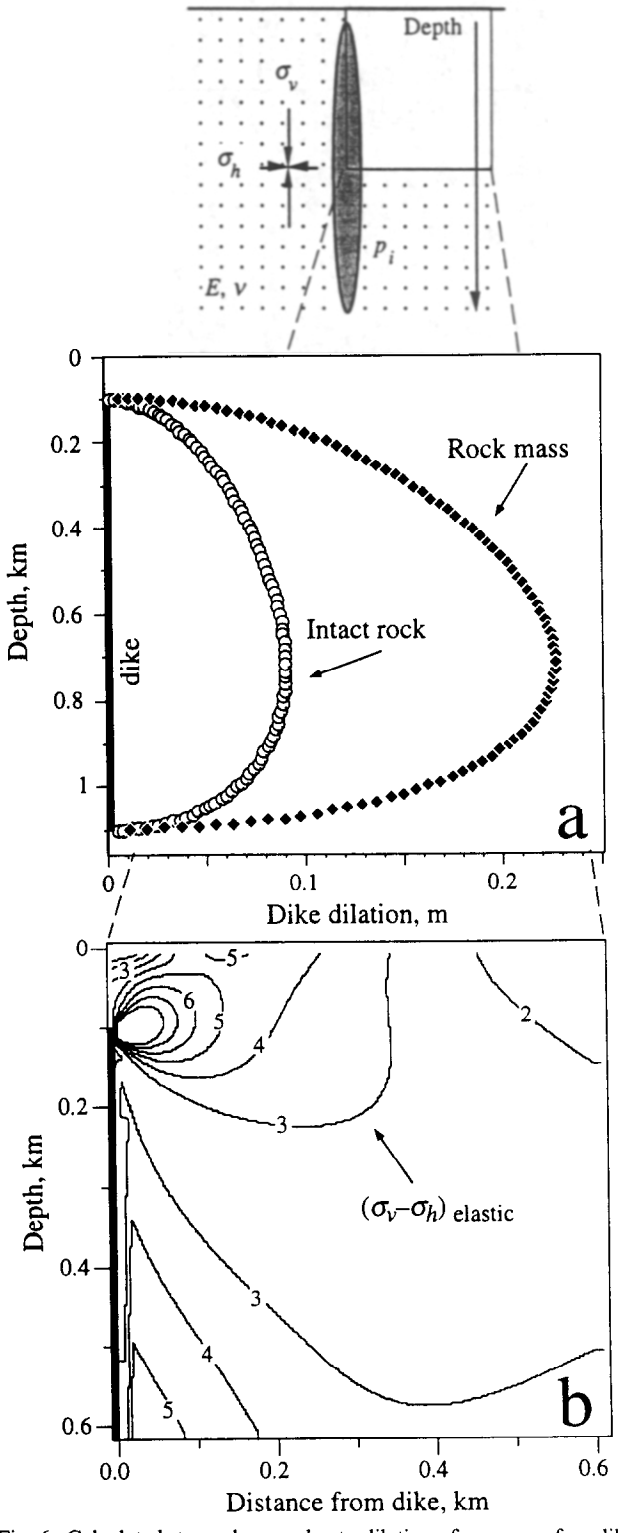

Fig. 6. Calculated stress changes due to dilation of a near-surface dike (inset). (a) Dilation across vertical dike due to magma pressure for intact rock and rock mass. (b) Contoured values of inhomogeneous elastic stress state ($\sigma_v - \sigma_h$) after dilation; note large differential stresses near the surface.

The occurrence of jointing or faulting due to dike dilation is considered by relating the stresses induced by dike dilation to the tensile or shear strength of the surrounding rock (e.g. Schultz & Watters 1995). Changes in differential stress ($\sigma_v - \sigma_h$) due to dike dilation, shown in Fig. 6(b), suggest the locations of potential failure (e.g.

at the surface for distances between 0.1 and 0.2 km away from the dike), but only if the stresses exceed the strength of the near-surface rocks (Fig. 7). Three possible idealizations for the strength of near-surface rock are considered: intact, pervasively fractured (strength given by joint friction only, Byerlee's rule), and Hoek–Brown rock mass. A critical value of differential stress, calculated as the ratio of elastic stresses to rock strength (Fig. 7, top), succinctly illustrates areas of potential failure (Schultz & Zuber 1994). Dike dilation in the intact basalt (Fig. 7a) is insufficient to cause failure in surrounding rock in either tension or shear. The largest value of the critical stress ratio for the intact rock, <0.2, demonstrates that a different strength criterion is necessary to predict dike-related jointing. Widespread faulting is predicted by using the simple joint-strength criterion (Byerlee's rule, Fig. 7b); jointing is not permitted, given that the joint Mohr envelope intersects the origin (Fig. 1). The prediction of faulting, rather than jointing, is not supported by the observations of initial tensile cracking at the surface near dikes (Mastin & Pollard 1988) in basaltic rock masses. Failure in tension across subvertical planes is predicted by using the rock-mass criterion (Fig. 7c) for levels of driving stress at or below those used in the analysis. The peak value of critical stress ratio (asterisks in Fig. 7b & c) where failure should first occur is located about 0.13 km away from the dike plane, or slightly greater than the depth to the dike top, in agreement with previous determinations (Mastin & Pollard 1988). Of the three strength criteria, the Hoek–Brown rock-mass criterion both predicts the initial failure (joints) and represents the fractured nature of the near-surface rocks. Nucleation of normal-fault displacements on the newly formed joints (Mastin & Pollard 1988, Rubin 1992) reflects the continued evolution of inhomogeneous near-surface stresses (Rubin 1995, Fig. 6b) that require localized assessments of failure criteria as the rocks deform inelastically to larger finite strains.

CONCLUSIONS

Fractures having a variety of sizes are present in most rock units. These fractures are associated with marked reductions in strength properties and moduli of rock masses relative to an unfractured hand sample or core. Rock-mass tensile, compressive, and cohesive strengths are all reduced by as much as a factor of ten from their intact-rock values, and the rock-mass deformation modulus is reduced by perhaps a factor of two from the

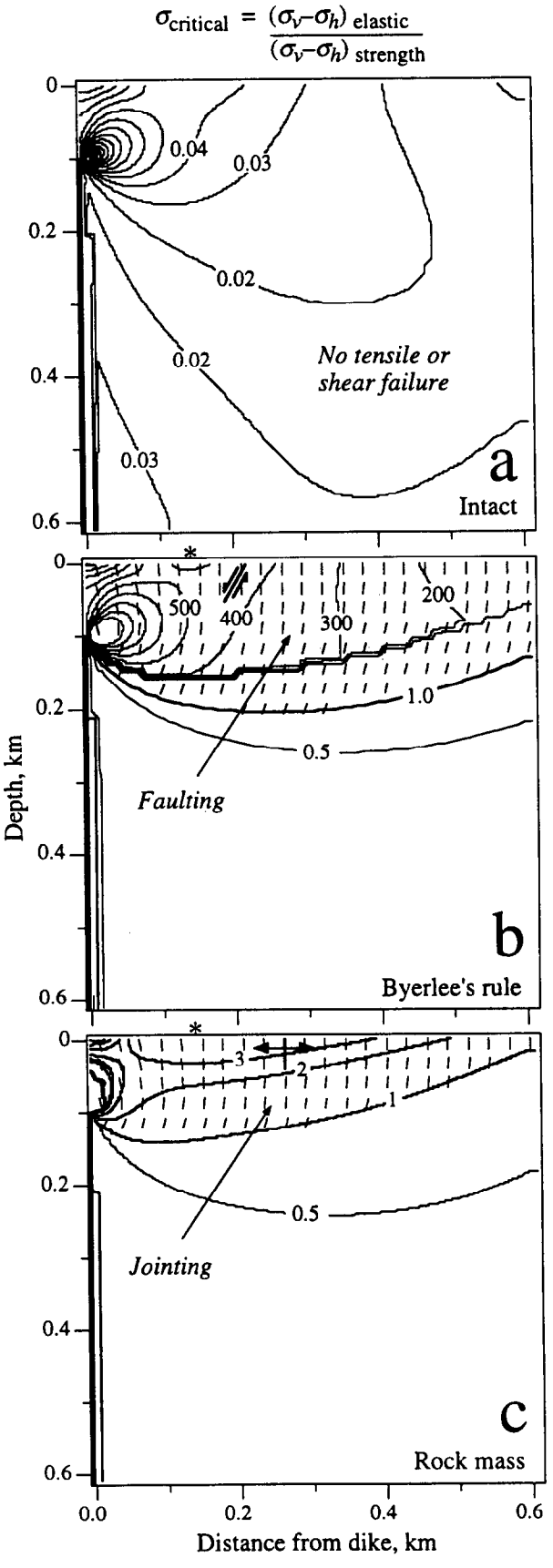

Fig. 7. Areas of predicted failure of near-surface rock due to dike dilation. (a) Intact basalt, $T_0 = -15$ MPa, friction coefficient 0.8; (b) joint-strength criterion for fractured basalt, $T_0 \approx 0$ MPa, friction coefficient 0.6; (c) rock-mass criterion, RMR = 65. Shaded regions denote predicted failure where critical stress ratio $\sigma_{critical} > 1.0$; asterisks indicate location of maximum values of $\sigma_{critical}$. Tick marks in (b) and (c) show orientations of greatest compressive local principal stress; normal faults in (b) would be oriented at $\pm 30°$ to this stress direction; dilatant cracks (joints, fissures) in (c) would be oriented parallel to this stress direction. Failure would occur first in areas of greatest $\sigma_{critical}$.

corresponding Young's modulus. An example of stresses and rock failure associated with igneous dike dilation demonstrates the utility of a rock-mass strength criterion for fractured near-surface rocks. Comparison of the scale of a particular problem relative to the scale of the fracture network is a natural prerequisite to choosing appropriate strength and deformation properties in regions of active crustal and near-surface tectonics.

Acknowledgements—I thank Atilla Aydin for introducing me to the complexities of joint and fault systems, and Bob Watters, Tom Watters, and Rich Schweickert for discussions on rock masses and failure criteria. Reviews by Paul Karabinos, Steven Wojtal, and an anonymous referee, and comments on various drafts by Don Secor, Steve Martel, Jason Moore, Paul Piscoran, and Edward Wellman led to significant improvements in this paper. The work was supported by grants from NSF (EAR-9105818), NASA's Planetary Geology and Geophysics Program, and the U.S. Department of Energy's Yucca Mountain Project, which are gratefully acknowledged.

REFERENCES

Amadei, B., Swolfs, H. S. & Savage, W. Z. 1988. Gravity-induced stresses in stratified rock masses. *Rock Mech. Rock Engng.* **21**, 1–21.

Angelier, J. 1989. From orientations to magnitudes in paleostress determinations using fault slip data. *J. Struct. Geol.* **11**, 37–50.

Aydin, A. 1988. Discontinuities along thrust faults and the cleavage duplexes. *Geometries and Mechanisms of Thrusting, with Special Reference to the Appalachians* (edited by Mitra, G. & Wojtal, S.). *Spec. Pap., Geol. Soc. Am.*, **222**, 223–232, Boulder, Colorado.

Barton, N. 1990. Scale effects or sampling bias? *Scale Effects in Rock Masses* (edited by Cunha, A. P.). Balkema, Rotterdam. 31–55.

Bieniawski, Z. T. 1989. *Engineering Rock Mass Classifications: A Complete Manual for Engineers and Geologists in Mining, Civil, and Petroleum Engineering*, Wiley & Sons, New York.

Brady, B. H. G. & Brown, E. T. 1992. *Rock Mechanics for Underground Mining*, George Allen & Unwin, London.

Broch, E. & Franklin, J. A. 1972. The point load strength test. *Int. J. Rock Mech. Min. Sci.* **9**, 669–697.

Brown, E. T. & Hoek, E. 1988. Determination of shear failure envelope in rock masses. *J. Geotech. Div., Am. Soc. Civ. Eng.* **114**, 371–376.

Byerlee, J. 1978. Friction of rocks. *Pure & Appl. Geophys.* **116**, 615–626.

Crouch, S. L. & Starfield, A. M. 1983. *Boundary Element Methods in Solid Mechanics*, George Allen & Unwin, London.

Deere, D. U. 1963. Technical description of cores for engineering purposes. *Rock Mech. Eng. Geol.* **1**, 16–22.

Goodman, R. E. 1995. Block theory and its application *Rock Mechanics: Proceedings of the 35th U.S. Symposium* (edited by Daemen, J. J. K. & Schultz, R. A.). Balkema, Rotterdam. 3–15.

Goodman, R. E. & Shi, G. 1985. *Block Theory and its Application to Rock Engineering*, Prentice-Hall, New Jersey.

Griffith, A. A. 1921. The phenomena of rupture and flow in solids. *Phil. Trans. Roy. Soc. Lond.* **A221**, 163–197.

Heuzé, F. E. 1980. Scale effects in the determination of rock mass strength and deformability. *Rock Mech.* **12**, 167–192.

Hoek, E. 1983. Strength of jointed rock masses. *Twenty-third Rankine lecture. Géotechnique* **33**, 187–223.

Hoek, E. & Brown, E. T. 1980. Empirical strength criterion for rock masses. *J. Geotech. Div., Am. Soc. Civ. Eng.* **106**, 1013–1035.

Horii, H. & Nemat-Nasser, S. 1985. Compression-induced microcrack growth in brittle solids: Axial splitting and shear failure. *J. geophys. Res.* **90**, 3105–3125.

Jaeger, J. C. & Cook, N. G. W. 1979. *Fundamentals of Rock Mechanics*, third edition, Chapman & Hall, London.

Kachanov, M. 1992. Effective elastic properties of cracked solids: Critical review of some basic concepts. *Appl. Mech. Rev.* **45**, 304–335.

Kohlstedt, D. L., Evans, B. & Mackwell, S. J. 1995. Strength of the lithosphere: Constraints imposed by laboratory measurements. *J. geophys. Res.* **100**, 17587–17602.

Kulhawy, F. H. 1975. Stress deformation properties of rock and rock discontinuities. *Eng. Geol.* **9**, 327–350.

Lin, M., Hardy, M. P., Agapito, J. F. T. & Assoc. & Bauer, S. J. 1993. Rock mass mechanical property estimations for the Yucca Mountain site characterization project. Albuquerque, New Mexico, Sandia National Laboratories report, *SAND92-0450*.

Marone, C. 1995. Fault zone strength and failure criteria. *Geophys. Res. Lett.* **22**, 723–726.

Mastin, L. G. & Pollard, D. D. 1988. Surface deformation and shallow dike intrusion at Inyo Craters, Long Valley, California. *J. geophys. Res.* **93**, 13221–13236.

Patton, F. D. 1966. Multiple modes of shear failure in rock. *Proc. 1st Int. Congr. Rock Mech.* **1**, 509–513.

Plumb, R. A. 1994. Variations of the least horizontal stress magnitude in sedimentary rocks. *Rock Mechanics: Models and Measurements, Challenges from Industry* (edited by Nelson, P. P. & Laubach, S. E.). Balkema, Rotterdam. 71–78.

Pollard, D. D. & Aydin, A. 1988. Progress in understanding jointing over the past century. *Bull. geol. Soc. Am.* **100**, 1181–1204.

Priest, S. D. 1993. *Discontinuity Analysis for Rock Engineering*, Chapman & Hall, London.

Priest, S. D & Hudson, J. A. 1981. Estimation of discontinuity spacing and trace length using scanline surveys. *Int. J. Rock Mech. Min. Sci. & Geomech. Abstr.* **18**, 183–197.

Rubin, A. M. 1992. Dike-induced faulting and graben subsidence in volcanic rift zones. *J. geophys. Res.* **97**, 1839–1858.

Rubin, A. M. 1995. Propagation of magma-filled cracks. *Ann. Rev. Earth Planet. Sci.* **23**, 287–336.

Scholz, C. H. 1990. *The Mechanics of Earthquakes and Faulting*, Cambridge, University Press, New York.

Schultz, R. A. 1988. Stress intensity factors for curved cracks obtained with the displacement discontinuity method. *Int. J. Fract.* **37**, R31–R34.

Schultz, R. A. 1992. Mechanics of curved slip surfaces in rock. *Eng. Analyt. Bound. Elem.* **10**, 147–154.

Schultz, R. A. 1995. Limits on strength and deformation properties of jointed basaltic rock masses. *Rock Mech. Rock Engng.* **28**, 1–15.

Schultz, R. A. & Li, Q. 1995. Uniaxial strength testing of nonwelded Calico Hills tuff, Yucca Mountain, Nevada. *Eng. Geol.* **40**, 287–299.

Schultz, R. A. & Watters, T. R. 1995. Elastic buckling of fractured basalt on the Columbia Plateau, Washington State. *Rock Mechanics: Proceedings of the 35th U.S. Symposium* (edited by Daemen, J. J. K. & Schultz, R. A.). Balkema, Rotterdam. 855–860.

Schultz, R. A. & Zuber, M. T. 1994. Observations, models, and mechanisms of failure of surface rocks surrounding planetary surface loads. *J. geophys. Res.* **99**, 14691–14702.

Segall, P. 1984. Rate-dependent extensional deformation resulting from crack growth in rock. *J. geophys. Res.* **89**, 4185–4195.

Sibson, R. H. 1994. An assessment of field evidence for Byerlee friction. *Pure & Appl. Geophys.* **142**, 645–662.

Walsh, J. B. 1965. The effect of cracks on the uniaxial compression of rocks. *J. geophys. Res.* **70**, 399–411.

APPENDIX

Description of RMR categories

1. *Strength of intact rock.* This index property, used to scale the Hoek–Brown Mohr envelope, is determined either in the laboratory from uniaxial compression tests or in the field from point-load tests of 50-mm diameter core (Broch & Franklin 1972).

2(a). RQD, *rock quality designation* (Deere 1963), is defined as the percentage of intact core in lengths greater than twice the core diameter. Core lengths typically range from 1 to 4 m and core fragments shorter than 0.1 m (4 in) are commonly excluded (Priest 1993). RQD samples the small-scale (<1 m) population of fracture spacings.

2(b). *Spacing of discontinuities* refers to macrocracks, faults, bedding planes, and other surfaces typically observed at larger, outcrop scales. An average or representative spacing is measured for the particular fractured domain.

2(c). *Condition of discontinuities.* Field observations pertinent to fracture strength include: *Roughness* and nature of asperities on fracture surfaces; the fracture-surface topography increases joint frictional resistance as the degree of interlocking and contact increases. Common types of asperities of mechanical significance encompass joint topography (e.g. plumose structure, twist hackles), fault

topography (e.g. slickensides, steps, undulations), and bedding plane topography (e.g. load casts, stratigraphic irregularities). Separation refers to the opening displacement across fractures; it controls the degree of interlocking of opposing fracture walls and the amount of fluid that can flow through the fracture. The amount of gouge may increase with the separation. *Continuity* of discontinuities is associated with the relative scales of fracturing and exposure; a continuous fracture is at least as long as the dimension of the exposure. *Weathering* of wall rock along discontinuity surfaces is classified as (a) Unweathered/fresh: no visible signs of weathering are apparent; (b) Slightly weathered: discontinuity surfaces are stained or discolored; may contain thin mineral fillings; discoloration of wall rock extends to $<20\%$ of discontinuity spacing; (c) Moderately weathered: discoloration extends farther into wall rock than 20% of spacing; fillings of altered minerals likely; (d) Highly weathered: discoloration extends throughout entire rock mass; rock material partly friable; (e) Completely weathered: rock totally discolored and friable, with external appearance similar to a soil. More detailed charts are available (Bieniawski 1989) for a finer delineation of the ratings for this broad category.

3. *Groundwater conditions* may contribute to a pore-fluid pressure, wall rock alteration, gouge formation, and changes in the stability of frictional sliding.